



A computational approach to unraveling TLR signaling in murine mammary carcinoma



Chun Wai Liew^a, Tiffany Phuong^b, Carli B. Jones^b, Samantha Evans^b, Justin Hoot^b, Kendall Weedling^b, Damarcus Ingram^b, Stacy Nganga^b, Robert A. Kurt^{b,*}

^a Department of Computer Science, Lafayette College, Easton, PA 18042, USA

^b Department of Biology, Lafayette College, Easton, PA 18042, USA

ARTICLE INFO

Keywords:

Breast cancer
Computer modeling
TLR
TAB3
NFκB
IRAKM

ABSTRACT

We developed an agent-based model to simulate a signaling cascade which allowed us to focus on the behavior of each class of agents independently of the other classes except when they were in physical contact. A critical piece was the ratio of the populations of agents that interact with one another, not their absolute values. This ratio reflects the effects of the density of each agent in the biological cascade as well as their size and velocity. Although the system can be used for any signaling cascade in any cell type, to validate the system we modeled Toll-like receptor (TLR) signaling in two very different types of cells; tumor cells and white blood cells. The iterative process of using experimental data to improve a computational model, and using predictions from the model to design additional experiments strengthened our understanding of how TLR signaling differs between normal white blood cells and tumor cells. The model and experimental data showed that some of the differences between the tumor cells and normal white blood cells were related to NFκB and TAB3 levels, and also suggested that tumor cells lacked IRAKM-dependent feedback inhibition as a negative regulator of TLR signaling. Finally, we found that these different cell types had distinctly different responses when exposed to two signals indicating that a more biologically relevant model and experimental system should address activation of multiple interconnected signaling cascades, the complexity of which further reinforces the need for a combined computational and molecular approach.

1. Introduction

There are several approaches that are commonly used to model complex cell signaling cascades including mathematical and agent-based systems [1–5]. These types of systems are extremely useful because they allow simulations to be run and data to be generated, and the results can be validated against experimental results. Here we developed an agent-based model to simulate a signaling cascade which allowed us to focus on the behavior of each class of agents independently of the other types of agents except when they were in physical contact. A critical piece was the ratio of the populations of agents that interact with one another, not their absolute values. This ratio reflects the density of each agent in the biological cascade as well as their size and velocity. We also developed a tool [6] that could be used to generate agent-based simulation models of signaling cascades. The tool does not require the user to have programming knowledge or skills and can be used by biologists who have

knowledge and understanding of the cascades. The biologist has to provide the tool with a description of the signaling cascade which is used to generate a NetLogo program which is then executed to generate simulation results. The tool has the advantage of allowing biologists to focus on model construction rather than programming and also greatly speeds up the process of developing an executable model. The modeler specifies the populations, generates the simulation results, and compares them to the lab results as well as past simulation results. Although the system can be used for any signaling cascade in any cell type, to validate the system we modeled the Toll-like receptor (TLR) signaling cascade in two very different cell types; tumor cells and white blood cells.

TLR signaling contributes to tumor progression, and yet TLR agonists are also currently being evaluated for cancer immunotherapy. Because we lack a complete understanding of how TLR agonists differentially impact tumor cells and white blood cells, and because this lack of understanding can have serious implications if TLR signaling is modulated

Abbreviations: IRAKM, interleukin 1 receptor kinase 3; TAB3, TGF-beta activated kinase 1/MAP3K7 binding protein 3; TLR, toll-like receptor; NFκB, nuclear factor κB.

* Corresponding author.

E-mail address: kurtr@lafayette.edu (R.A. Kurt).

<https://doi.org/10.1016/j.complbiomed.2017.12.013>

Received 6 September 2017; Received in revised form 16 December 2017; Accepted 16 December 2017

in a tumor setting where both types of cells are present, we wanted to gain a deeper understanding of how this signaling cascade differed between these two cell types. To study the relationship between TLR signaling and cancer we focused on the TLR4 signaling cascade in 4T1 murine mammary carcinoma because it is a highly aggressive and metastatic tumor often used as a model for stage IV disease in patients with breast cancer [7]. CCL2 was assessed not only because it is downstream of the TLR4 signaling cascade, but also because CCL2 expression has been correlated with breast cancer progression in humans [8–10]. DC were used as a control because they serve as excellent antigen presenting cells, they make a strong response to TLR agonists, their signaling cascades have been well described, and TLR agonist treated DC are being used for cancer immunotherapy [11,12].

The model that we constructed is an agent-based model where each component is represented as an agent [13]. We took this approach rather than using a more mathematically oriented approach that would require information such as diffusion speed and size of components, as well as equations to describe the interactions between the components. We did not possess much of this information about the components and the agent-based approach allowed us to create computational models that would let us explore our understanding of the interactions. The only information necessary with our agent-based approach was a set of rules [14] describing how each component (agent) moves in 3D space and how each component behaves when it interacts with another component in the signaling cascade.

The tradeoff with the agent-based approach is that it may require carrying out more simulations before one can determine the conditions (relative populations of the agents) that yield simulation results that match the lab (experimental) results. Yet, our model allows a user to change the level of any of the TLR signaling proteins and quickly determine how the altered protein levels influence CCL2 expression. As a result, our model can be used to rank the importance of any protein in the signaling cascade. For instance, the model can be used to predict what happens in response to a TLR agonist if any of the TLR signaling proteins are up- or down-regulated. We learned that although the tumor cells expressed lower levels of many of the TLR signaling components than DC they did not exhibit lower TLR signaling capabilities. The model and experimental data indicated that this was related to NF κ B and TAB3 levels, and a lack of IRAKM-dependent negative feedback signaling in the tumor cells. Moreover, we found that the tumor cells and DC differed in response when exposed to two concurrent signals. Along this same line, Moreno et al., [15] recently reported that activation of two TLR signaling cascades had a different outcome than activation of a single TLR signaling cascade. They reported that dual TLR7 and TLR9 signaling impaired NF κ B activation. And, Han et al. [16] recently reported crosstalk between the hypoxia-inducible factor -1 (HIF-1), and TLR3 and TLR4 signaling cascades. These data, along with our findings here, suggest that a greater understanding of signaling differences between tumor cells and normal white blood cells should take into account multiple interconnected signaling cascades, and reinforces the need for a combined experimental and computational approach as investigators move away from studying single signaling cascades in isolation.

2. Materials and methods

2.1. Cells and mice

4T1 murine mammary carcinoma were maintained in complete RPMI (cRPMI) (RPMI 1640, Lonza, Walkersville, MD) supplemented with 10% heat-inactivated fetal bovine serum (Lonza), glutamine (2 mM, Lonza), penicillin (100U/mL, Lonza), streptomycin (100 μ g/mL, Lonza), nonessential amino acids (Sigma, St. Louis, MO), 2-mercaptoethanol (5×10^{-5} M, Sigma), and sodium pyruvate (1 mM, Lonza). DC were generated from femurs and tibias from Balb/c mice and were cultured at 1×10^6 cells/ml in cRPMI with GM-CSF (20 ng/ml, Peprotech, Rocky Hill, NJ) and IL-4 (10 ng/ml, Peprotech) with one ml/well in 24-well

tissue culture dishes (Costar, Fisher, Pittsburgh, PA). The media with GM-CSF and IL-4 was replaced every 2–3 days. After 7–8 days, CD11c⁺ DC were purified using CD11c microbeads and MS positive selection columns (Miltenyi Biotec, Auburn, CA). Balb/c mice were bred on site and housed in a thoren caging system (Thoren Caging Systems Inc., Hazleton, PA). Food and water were provided *ad libitum*. All mice were used in accordance with an Institutional Animal Care and Use Committee approved protocol that followed the guidelines for ethical conduct in care and use of animals.

2.2. Treatment with TLR agonist

Lipopolysaccharide (LPS) from *Escherichia coli* K12 (Invivogen, San Diego, CA) was used as a TLR4 agonist. Stocks were prepared in sterile water, aliquoted and stored at -20°C in sterile microcentrifuge tubes. For TLR agonist treatment, 1×10^6 tumor cells or DC were cultured in 24 well culture plates at 1ml/well with or without the TLR agonist and incubated at 37°C , 5% CO₂. Twenty four hours later RNA was collected from the cells and supernatants were harvested to assess CCL2 gene or protein expression respectively. To assess IL-1 β expression the cells were treated for 24 h with LPS and then another 24 h with ATP (Invivogen) or nigericin (Invivogen) before harvesting supernatants.

2.3. Quantitative reverse transcriptase polymerase chain reaction

Gene expression was analyzed by qRT-PCR. For this purpose, RNA was isolated from approximately 1×10^6 cells using the Aurum Total RNA Mini Kit (Bio-Rad Laboratories, Hercules, CA) according to manufacturer's instructions. Briefly, the cells were lysed, RNA was bound to the column, treated with DNase, and following several washes, RNA was eluted and stored at -20°C . Complementary DNA was generated using the iScript cDNA synthesis kit (Bio Rad Laboratories). For this purpose 15ul RNA, 4ul 5x iScript buffer and 1ul iScript reverse transcriptase were combined in a 0.5 ml microcentrifuge tube and placed in a thermal cycler (MiniCycler, MJ Research Watertown, MA). The reaction conditions consisted of 25°C for 5 min, 42°C for 30 min, and then 85°C for 5 min. All samples were stored at -20°C prior to qRT-PCR. An aliquot (0.5ul) of cDNA was amplified in a reaction with 1x iQ SYBR Green Supermix (Bio-Rad Laboratories) and 200 nM gene specific primers. The reaction conditions consisted of 40 cycles of a two-step PCR reaction with 94°C for 10 s, and 68°C for 30 s on an iQ5 Real Time PCR Detection System (Bio-Rad Laboratories). Gene specific primers (Table 1) were synthesized by Integrated DNA Technologies (Coralville, IA) and analyzed for specificity with the NCBI Blast Program. The housekeeping gene *gapdh* was used to establish normalized expression ($\Delta\Delta\text{C}_T$).

2.4. ELISA

Supernatants harvested from cells were centrifuged at $400 \times g$ to remove particulate matter and stored at -20°C . For analysis of culture supernatants CCL2 and IL-1 β specific quantikine colorimetric sandwich ELISAs were used according to manufacturer's instructions (R&D Systems, Minneapolis, MN).

2.5. Western blot

To analyze protein expression 5×10^6 cells were washed three times with ice-cold phosphate buffered saline (PBS), resuspended in 150ul of buffer A (10 mM Hepes (Sigma), 10 mM KCl (Sigma), 0.1 mM EDTA (Sigma), 0.1 mM EGTA (Sigma)), supplemented with the protease inhibitors aprotinin, leupeptin, chymostatin, and pefabloc (Roche Molecular Biochemicals, Indianapolis, IN) and placed on ice. Following a 15 min incubation, 10ul of 10% Nonidet P-40 (Sigma) was added. The samples were vortexed for 10 s, and centrifuged $15,000 \times g$ at 4°C for 1 min. The pellets were washed one time with buffer A and then resuspended in 75ul buffer B (25% glycerol, 20 mM Hepes (Sigma), 0.4 M

Table 1
Gene specific primers.

gene	forward primer 5' to 3'	reverse primers 5' to 3'
gapdh	cttcctgttctaccaccaatgt	gcctctcaccacctcttgatg
TLR4	agtgcctcccttcaactctg	caataacctccggctcttgga
MYD88	cctgaccaccactcgagttgt	tgcgcgactcagctcttca
IRAK2	tggagtgaaagcagatgtctcca	ttgaaggccaagggccacacc
IRAK4	tccgtaatgcctatgccgaagcta	tggaaacagatgtcctgga
TRAF6	tgcaaggagaatgatgacgccactc	gctgcatgactctcctggtt
TAK1	tgacaggcacaagccagattgaga	tgagtgtctgtagggcggacaaga
TAB1	atggctgtctggcagctcttc	tcctcttctcgggtgtgtgt
TAB2	cctcattggtcaacagccagacct	atctctcgggtggactgg
TAB3	gttctctctcagattggcatcc	ggcatggaacctcacaatcagt
IKKa	cctgcatatgacgccatcttg	tcagccaccaactcctgca
IKKb	tggcaacaatcaggcgacagg	aggcaccagcggctctcttctt
IKKg	cggaaagtggctcagttgca	ttgctggagctgttgcctcagat
p50	tcgcttggcatcaccat	cggccagcaacatcttcacatc
p52	acgagaacggagacacgccact	tctggctgacaggtgtgtgag
p65	tcaccggcctcaccatg	ttgtccaggctcctcttca
cREL	tggtgtcagcacttgatgcat	cagagccgagtagatgcatgtgac
RELB	tgccattgagcgaagatcca	tccatgctggctgagatgctc
JUN	aaggcagagagaaagcgcata	ctgagcatgttgcctgga
FOS	agcgcagagatcggcagaa	attccggcactgtgctca
ATF2	cagccagccactcactacagaa	ctgctcttctcagcggcact
STAT5	tggcagaaccggcagcagat	tcctgtagtggcgttgac
CEPBB	caaggccaagaagcgggtggac	cttgtgtcgtctccaggtg
ETS1	tgagcgtgctcctcacta	tacatcagcatggctgca
CCL2	tcattctctggcctcctgt	ctcatgggatactctgtgtg
MYD88s	gcatcgcgcggaaacttt	gccgatcatctcctgca
RP105	ctcggctgttggaggctctctgt	caggtgagtgctgttaggtccagt
IRAKM	tggcgaccctcctatgaa	ttggcctctggtccacaca

NaCl (Sigma), 1 mM EDTA (Sigma), 1 mM EGTA (Sigma)) supplemented with the protease inhibitors aprotinin, leupeptin, chymostatin, and pepabloc (Roche Molecular Biochemicals), and then sonicated for 30 s. After a 10 min centrifugation at 15,000 × g the supernatants containing the nuclear proteins were transferred to new tubes, NuPAGE LDS sample buffer was added, and the samples were stored at −20 °C. For analysis SDS PAGE gels (12.5%, Fisher) were loaded with 15 µL of proteins, electrophoresed, and transferred to PVDF membranes (Fisher). The membranes were blocked at room temperature in PBS with 5% powdered milk (Carnation) and 0.05% Tween 20 (Sigma) for 2 h. Primary antibodies (10 µg) specific for histone 3, NFκB p50, p52, p65, cREL and RELB (Santa Cruz Biotechnology, Santa Cruz, CA) were added, and the blots were incubated at room temperature for 1 h followed by an overnight incubation at 4 °C. After washing four times with blocking buffer, a horse-radish-peroxidase-conjugated secondary antibody (Santa Cruz) was added and the blots were incubated for 2 h at room temperature. Following four washes, proteins were visualized by enhanced chemiluminescence on a gel documentation system (Bio-Rad Laboratories). Densitometry data were normalized to actin and nuclear histone 3 levels which showed similar expression patterns.

2.6. RNA interference

Tumor cells were cultured in 24 well culture plates at 1×10^4 cells/well in cRPMI without antibiotics and incubated at 37 °C, 5% CO₂. Twenty four hours later the media was replaced and the cells were transfected with 80 pmole siRNA specific for NFκB p52, p65, RELB, IRAKM, or scrambled siRNA as a control (Santa Cruz) with 6 µl lipid transfection reagent (Santa Cruz). After another 24 h incubation the media was replaced and LPS (0, 1, 10, 100 ng/ml) was added. Cell supernatants or RNA were harvested 24 h later to assess CCL2 levels.

2.7. Computer programming and model

We developed an agent-based simulation model to simulate the TLR4 cascade. Each of the components of the model (TLR4, MYD88, IRAK2, etc.) were represented as a class of agents. The behavior of each class of agents was specified by a set of rules that described the behavior of the

agent under various circumstances, e.g., how it moves in 3 dimensions and what changes when it encounters (is in physical contact with) another agent of a different class.

The agent-based modeling approach (as compared to a mathematical modeling-based approach [4]) allowed us to (1) focus on the behavior of each class of agents independently of the other classes except when they were in physical contact, (2) develop a simulation model even though we did not have all of the specific data/knowledge about the agents, e. g, diffusion rates. The movement of the agents is similar to that of Brownian motion. Even though we did not have specific interaction rates for the agents, we computationally determined the effects of the cascade through simulations and compared them with experimental results from the lab. Through iterative trials, we determined the relative ratios of the agent populations in the model that led to results that matched those of the lab experiments. The ratios of the agent populations accounted for differences such as the size and velocity of the agents when determining how frequently interactions between agents occurred.

2.7.1. Using the model

For this specific cascade model, TLR4 was set in the cell surface, MYD88 and associated signaling proteins in the cytoplasm and the CCL2 gene in the nucleus. The signaling cascade began when LPS bound to TLR4 and was followed by subsequent protein-to-protein interactions leading to phosphorylation of the NFκB/IκBα complex. Once activated, NFκB entered the nucleus and bound to the CCL2 promoter inducing transcription.

The initial simulation model was built by hand (custom programming) and it was a tedious process with many places where bugs occurred. However, we gained knowledge about modeling cascades and we subsequently developed a tool [6] that could be used to generate agent-based simulation models of signaling cascades. The tool does not require the user to have programming knowledge or skills and can be used by biologists who have knowledge and understanding of the cascades. The biologist has to provide the tool with a description of the signaling cascade which is used to generate a NetLogo program which is then executed to generate simulation results.

The primary tasks of the modeler (biologist) are to (1) specify the model, and (2) to validate the simulation results against the experimental results. Specifying the model requires that the modeler decide which parts of the cascade (agents) are “essential” and have to be included in the model while other agents are left out. These decisions are crucial because they affect both the accuracy of the model (leaving out an essential agent renders the model invalid) and the efficiency with which results are derived (including too many agents greatly increases the computational time). Once the model is specified, the next step is to state the initial conditions. Primarily this step is concerned with specifying the initial population of each of the agents. This is done through the NetLogo interface where boxes have been created (with default values) for each of the agents. The critical piece is the ratio of the populations of agents that interact with one another, not their absolute values. This ratio reflects the effects of the density of each agent in the biological cascade as well as their size and velocity. The modeler specifies the populations, generates the simulation results, and compares them to the lab results as well as past simulation results. Results from the comparison are used to determine how to adjust the populations on the next simulation so as to generate results that are a better match for the lab results. This process is repeated until the modeler is satisfied.

2.7.2. Building the model

The process of constructing an agent based model of a biochemical cascade is similar to that of building a directed cyclic graph or network graph. Each node in the graph represents either a component or an interaction between two components. This results in the production of a new component and/or the participating components changing state. To build a model, the user (biologist) has to specify the components and the interactions in the cascade.

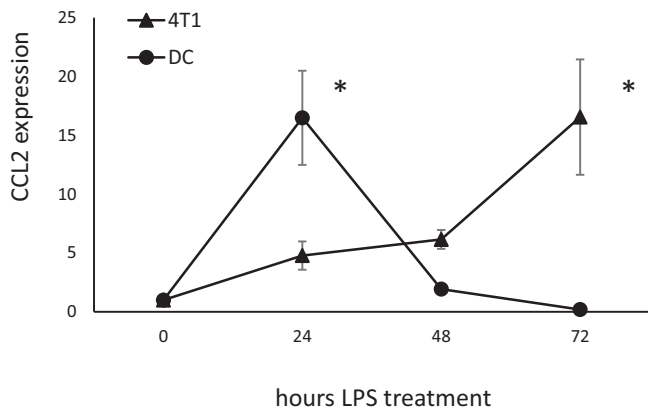


Fig. 1. 4T1 and DC elicit a distinct response to LPS. In order to determine how much CCL2 was produced by 4T1 and DC we quantified the amount of CCL2 produced by the cells following LPS treatment. For this purpose 4T1 and DC were treated with LPS (10 ng/ml) for 24–72 h and qRT-PCR was used to measure the amount of CCL2 mRNA produced by the cells. The data represent the average and standard error of at least three separate experiments. Where indicated (*) $p < .05$ using Student's *t*-Test relative to DC.

To start, the user describes all the components in the cascade by giving each one a unique name and a location (external to the cell, cell

membrane, cytoplasm, nucleus) and then selecting a shape and color so that it can be visually distinguished. The next step is to describe the interactions in the cascade by giving each one a unique name, the names of the participating components and the resulting component if any. In addition, the user has to specify any enabling or disabling (inhibitory) interactions. If there is a component that should travel to another location (e.g. from the cytoplasm into the nucleus) after an interaction, then a new component is added to the list of components and this new component in the nucleus is created as a result of the interaction.

The tool that we developed will then create a NetLogo program where the “world” is divided into the four spaces - outside the cell, cell membrane, cytoplasm, nucleus - and the component classes are instantiated in their specified spaces. During each simulation time step, each component will move in a random direction in the 3-D world. For each interaction in the model, the tool generates code that will check if instances of the specified components are physically adjacent and if they are, the pre-conditions are then validated (the enabling interactions have occurred and the disabling interactions have not). If all the conditions are met, the interaction happens and the components change state and new components are created as described by the interaction. In general, the participating components will maintain their new state for some pre-determined number of time steps and then revert to the original state. Created components will exist for a pre-determined number of time steps and then will decay.

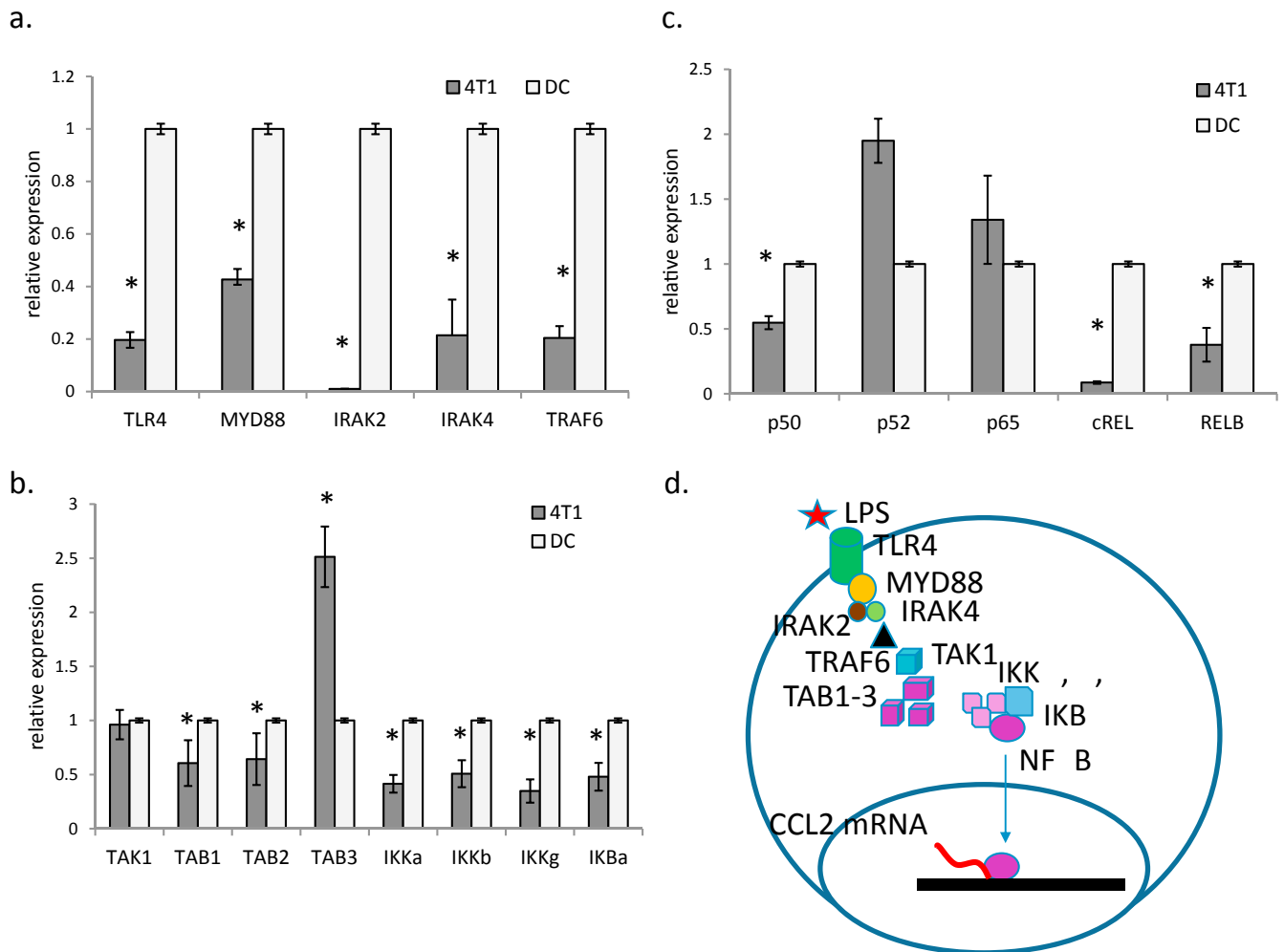


Fig. 2. Most of the genes encoding TLR signaling proteins were expressed at lower levels in 4T1 than DC. (a–c) Quantitative RT-PCR was used to analyze expression of genes encoding TLR signaling proteins from TLR4 through the NF κ B transcriptional factors. For all data *gapdh* was used as the reference gene and DC served as the control. The data represent the average and standard error of three separate experiments. Where indicated (*) $p < .05$ using Student's *t*-Test relative to DC. (d) A diagram of the signaling cascade from LPS binding to TLR through transcription of CCL2.

The tool has the advantage of allowing biologists to focus on model construction rather than programming and also greatly speeds up the process of developing an executable model. The tool is written in the Scala language (version 2.12.6) and runs on the Ubuntu (16.04) operating system. The executable NetLogo programs were generated for the NetLogo 6.0.1 environment.

3. Results

3.1. Tumor cells and DC exhibit a distinct response to a TLR4 agonist

To study the relationship between TLR signaling and cancer we focused on the TLR4 signaling cascade in 4T1 murine mammary carcinoma because it is a highly aggressive and metastatic tumor often used as a model for stage IV disease in patients with breast cancer [7]. CCL2 was assessed not only because it is downstream of the TLR4 signaling cascade, but also because CCL2 expression has been correlated with breast cancer progression in humans [8–10]. DC were used as a control because they serve as excellent antigen presenting cells, they make a strong response to TLR agonists, their signaling cascades have been well described, and TLR agonist treated DC are being used for cancer immunotherapy [11,12]. We found that DC made a strong initial response to the TLR4 agonist LPS at 24 h, and then the response decreased after 48 and 72 h of treatment (Fig. 1). On the contrary, the tumor cells exhibited a small response at 24 h, but then the response increased after 48 and 72 h of treatment (Fig. 1). These data showed that the tumor cells and DC responded in a

distinct manner to a TLR4 agonist. We combined a computational and molecular approach to pursue possible reasons for this difference.

3.2. Modeling the TLR signaling cascade

To construct a model of the TLR signaling cascade we quantitated mRNA levels encoding 18 different TLR signaling proteins using quantitative RT-PCR. The majority (14/18) of the genes examined were expressed at significantly greater levels by DC. The data showed that TLR4, as well as other signaling proteins located near the cell surface (MYD88, IRAK2, IRAK4 and TRAF6), were expressed at significantly greater levels by DC (Fig. 2a), while TAB3, NF κ B p52 and p65 were expressed at greater levels by 4T1 (Fig. 2b and c). How these components interact functionally in the cell and model is shown in Fig. 2d. Initially, the cascade would begin when LPS binds TLR4 which would then result in recruitment of the adaptor MYD88. Once MYD88 binds TLR4 then IRAK2 and IRAK4 are able to bind MYD88 resulting in recruitment and activation of TRAF6. The TRAF6/TAB/TAK complex can then inactivate the NF κ B inhibitor (IKBa) allowing NF κ B to enter the nucleus and transcribe CCL2. The relative gene expression levels from the qRT-PCR were used to create a NetLogo model. The input boxes allowed the numbers to be changed so that cellular responses to LPS with different levels of TLR signaling proteins could be modeled, and the sliders allowed the number of specific proteins recruited per signaling cascade to be adjusted.

Because there were so many proteins in the model we compared two different size worlds, each of which represented a single cell, to

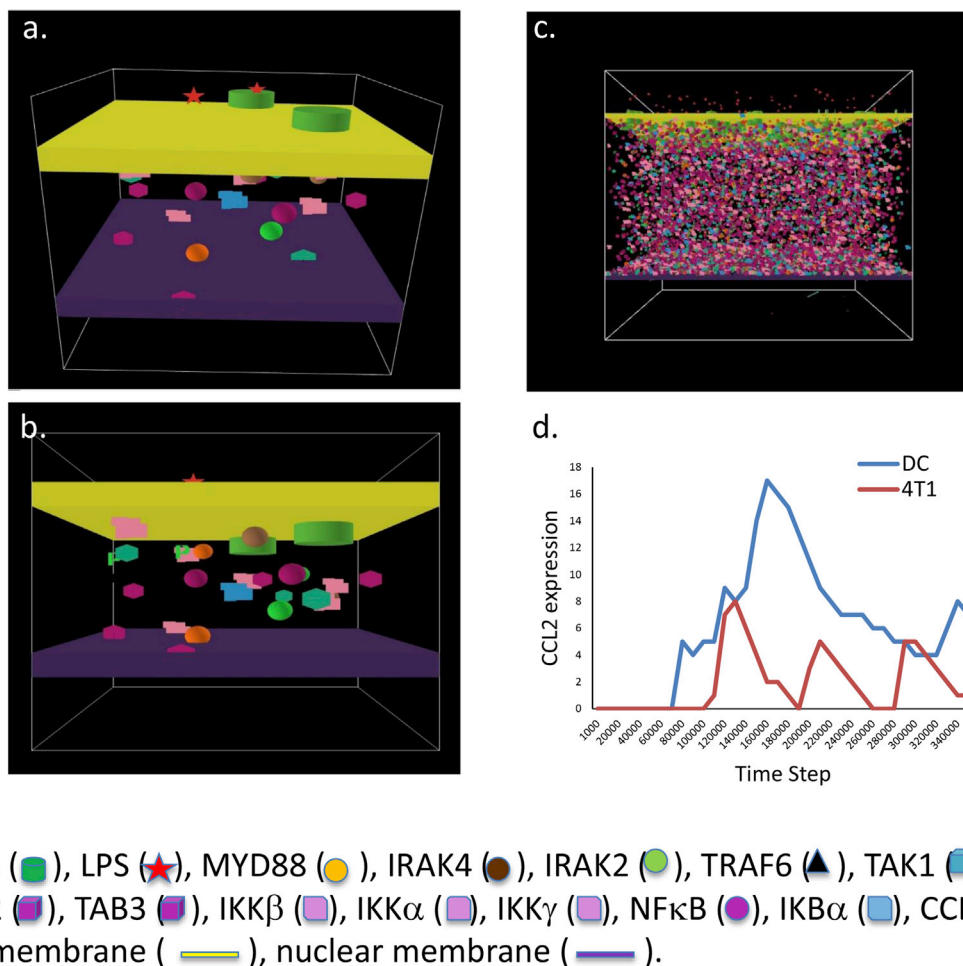


Fig. 3. The model. A simplified model (a, b) shows two TLR4 signaling cascades in the presence of two molecules of LPS. (c) We multiplied the relative gene concentration levels (qRT-PCR data) by 1000 to mimic cellular levels of TLR signaling proteins for the actual model. The model shows the outside of the cell where LPS interacts with TLR4 on the outer leaflet of the plasma membrane. The signaling cascades culminate in NF κ B entering the nucleus to transcribe CCL2. (d) The model was used to determine how much CCL2 could be produced by 4T1 and DC. Data for 350,000 time steps for each simulation is shown.

determine whether the density of the proteins affected the outcome of the simulation. 4T1 had a total of 9305 TLR signaling proteins in the cytoplasm and 190 TLR4 in the plasma membrane. DC had 13,000 TLR signaling proteins in the cytoplasm and 1000 TLR4 in the plasma membrane so that the numbers were relative to the qRT-PCR data (Fig. 2a–c). The volume of the big world ($200 \times 62 \times 64$) was three times larger than the volume of the small world ($70 \times 62 \times 64$). The big world had a protein concentration of 0.0117 proteins/unit³ in 4T1 and 0.0164 proteins/unit³ in DC, while the small world had a protein concentration of 0.0335 proteins/unit³ in 4T1 and 0.0468 proteins/unit³ in DC. In order to determine how much CCL2 could be produced by the 4T1 and DC models we ran each simulation for 500,000 steps. Snapshots of the model while running are shown in Fig. 3a–c. The model shows the outside of the cell where LPS interacts with TLR4 on the outer leaflet of the plasma membrane. The signaling cascades culminate in NFκB entering the nucleus to transcribe CCL2. Expression of CCL2 upon exposing the “cell” to LPS (running the model) indicated that there were no basic programming flaws and that the model was functional (Fig. 3d). The data showed that the size of the modeled world did not affect CCL2 expression (data not shown), yet data from the model (Fig. 3d) did not recapitulate data from the laboratory experiment (Fig. 1).

3.3. Assessing the importance of NFκB

Because elevated levels of NFκB have been associated with many tumors [17–19], and because NFκB is a transcriptional factor for CCL2 [20], we wanted to determine the extent to which NFκB levels were associated with TLR4-induced CCL2 expression by the tumor cells and whether modulating NFκB levels in the model would allow the modeling data to recapitulate the experimental data. To evaluate the importance of

NFκB for CCL2 production in the model we ran the simulation after altering NFκB levels in 4T1 and DC. Intriguingly, the tumor cells and DC responded differently to altered NFκB levels in the model. CCL2 expression by 4T1 was generally increased when NFκB levels were increased, whereas CCL2 expression by DC was generally decreased when NFκB levels were increased (Fig. 4a). These data showed that NFκB levels were important for CCL2 expression in the model, but that we could not modulate NFκB levels in a manner that would allow the data from the model to recapitulate the experimental data. Because of these results we further explored the importance of NFκB experimentally. Initially we confirmed that the mRNA levels found by qRT-PCR (Fig. 2c) were consistent with proteins levels. For this purpose we assessed the relative levels of NFκB p50, p52, p65, cREL and RELB by western blot (Fig. 4b). Densitometry analysis of the data revealed a pattern of protein expression similar to mRNA expression (Figs. 4c and 2c). RELB was the one exception which exhibited lower mRNA levels compared to the DC (Fig. 2c), but higher protein levels (Fig. 4c). To experimentally evaluate whether any of the NFκB proteins were important for CCL2 expression by the tumor cells we used RNA interference and found that targeting NFκB p65 led to a significant decrease in CCL2 expression following LPS treatment (Fig. 4d). Collectively, these data indicated that NFκB levels, as evaluated with the model and laboratory experiments, were important for CCL2 production, but that modulating NFκB levels could not help align the modeling data with the experimental data.

3.4. Additional improvements to the model

One protein that could be modulated to better align the modeling and experimental data was TAB3. When TAB3 levels were modulated in the 4T1 model we found that there was not much difference in CCL2

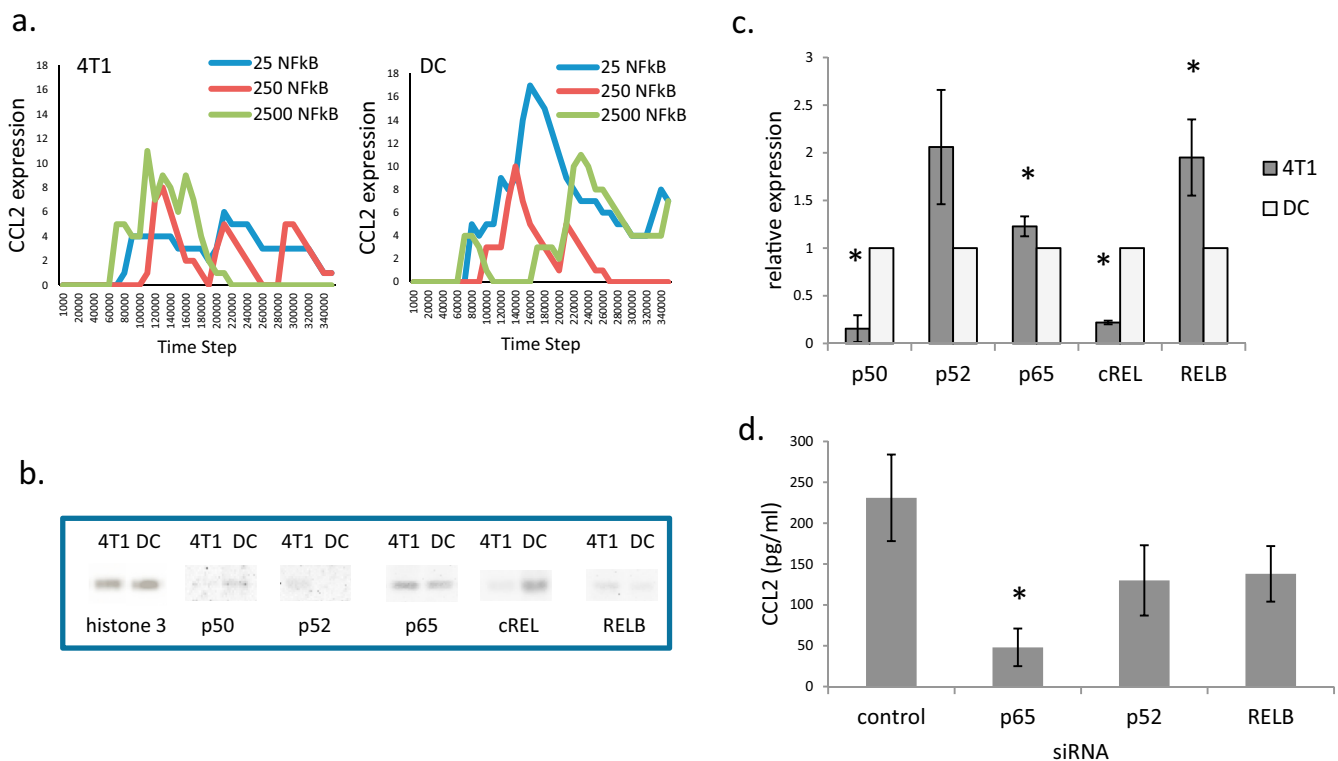


Fig. 4. The model and experimental data show the importance of NFκB for CCL2 production.

To evaluate the importance of NFκB levels in the model we ran the model after adjusting the level of this protein. (a) Reducing the level of NFκB from 2500 to 25 proteins in 4T1 resulted in a general decrease in CCL2 production, whereas reducing the level of NFκB from 2500 to 25 proteins in DC resulted in a general increase in CCL2 production. Western blot (b) and densitometry (c) were used to compare NFκB levels between 4T1 and DC from at least three separate experiments. (d) siRNA was used to determine the importance of NFκB p65, p52, and RELB in the response of 4T1 to LPS. Twenty four hours after siRNA transfection 4T1 were treated with 10 ng/ml LPS and supernatants were harvested 24 h later to quantify CCL2 levels by ELISA. Cells transfected with scrambled siRNA were used as a control. The data represent the average and standard error of at least three separate experiments. Where indicated (*) $p < .05$ using Student's *t*-Test relative to DC (c) or control (d).

expression except at the highest level of TAB3 (2500) for which there was no CCL2 expression (Fig. 5a). Modulating TAB3 levels in the DC model showed results similar to what was found when NF κ B levels were modulated in DC; increasing the level of TAB3 resulted in lower CCL2 expression (Fig. 5b). Moreover, when comparing the level of CCL2 expression when there was a high level of TAB3 in 4T1 and a low level of TAB3 in DC, which was similar to the experimental data (Fig. 2b), we

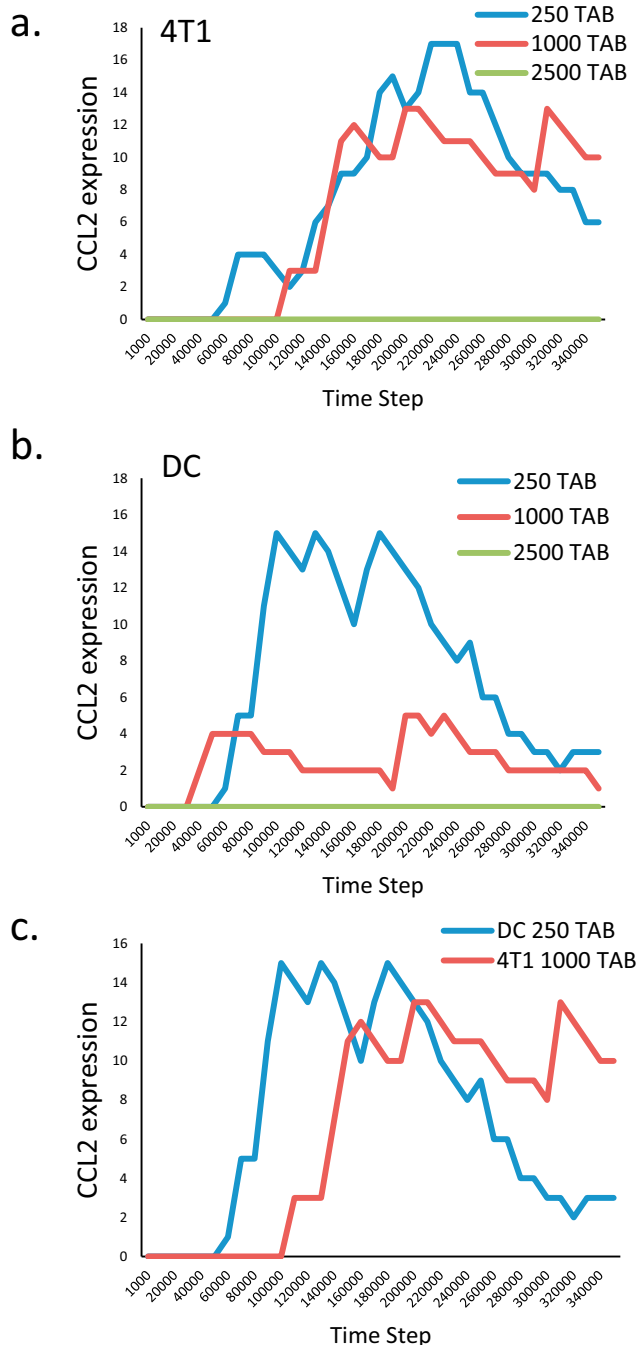


Fig. 5. Modulating TAB3 levels in the model helped align the modeling data with the experimental data. To evaluate the importance of TAB3 levels in the model we ran the model after adjusting the level of this protein. (a) 4T1 produced similar levels of CCL2 when TAB3 was set at 1000 or 250, but when the level was set at 2500 CCL2 expression was inhibited. (b) Reducing the level of TAB3 from 1000 to 250 proteins in DC resulted in an increase in CCL2 production, but when the level was set at 2500 CCL2 expression was inhibited. (c) The modeling data could recapitulate the experimental data when 4T1 TAB3 levels were set at 1000 and DC TAB3 levels were set at 250.

found that DC initially expressed more CCL2 than 4T1, and there was a delayed increase in CCL2 expression by 4T1 (Fig. 5c). These data from the model looked similar to the experimental data (Fig. 1) which also showed DC initially expressed more CCL2 than 4T1, and there was a delayed increase in CCL2 expression by 4T1. We also investigated whether modulating NF κ B levels with the new TAB3 levels could further improve the model and found that increasing NF κ B levels resulted in lower levels of CCL2 production for 4T1, and made the CCL2 levels rise and fall faster in DC. In short, modulating NF κ B levels could not improve the model beyond what is shown in Fig. 5c.

One final improvement to the model was to incorporate negative regulation of TLR signaling. To determine how to model negative regulation of TLR signaling we began with DC since they make a prototypical response to TLR agonists. We screened DC for expression of three possible negative regulators of TLR signaling; MYD88s, RP-105 and IRAKM. IRAKM expression increased 48–72 h following TLR4 agonist treatment; the pattern expected of a negative regulator (Fig. 6a). IRAKM was not expressed by the tumor cells even after 72 h of agonist treatment (Fig. 6b). Moreover, if IRAKM expression was blocked in DC with siRNA then after 72 h of LPS treatment the relative expression of CCL2 by DC was 15 ± 6.0 , similar to the relative expression of CCL2 by 4T1 which was 16 ± 4.9 (Fig. 6c). In short, inhibition of this negative regulator resulted in maintaining elevated levels of CCL2 expression. These data are consistent with the ability of IRAKM to function as a negative regulator of TLR signaling in DC, and suggest that this negative regulator was missing in the tumor cells. Incorporating IRAKM as a negative regulator further improved the ability of the model to recapitulate the experimental data. When IRAKM was added to the model DC initially expressed more CCL2 than 4T1, and then as CCL2 expression decreased in DC the CCL2 expression increased in 4T1 (Fig. 6d); results that were similar to the experimental data (Fig. 1).

3.5. Other factors not taken into account by the model

Although we included NF κ B in the model as a transcriptional factor for CCL2, in reality the CCL2 promoter includes binding sites for additional transcriptional factors. We investigated expression of other CCL2 transcriptional factors to delineate whether there were additional differences between the tumor cells and DC that we did not incorporate into the model. This analysis revealed that 4T1 expressed significantly more mRNA encoding JUN, FOS and ETS1 than DC, and significantly less STAT5 and CEPBb than DC (Fig. 7a).

Finally, we investigated a combination of two signaling cascades and expression of another pro-inflammatory cytokine. For this purpose we stimulated 4T1 and DC with the TLR4 agonist LPS followed by either nigericin or ATP to activate inflammasome signaling and assessed production of IL-1 β . In this case DC produced significantly more IL-1 β than 4T1 (Fig. 7b). Assessing IL-1 β expression in the tumor cells over a range of times (24–120 h) failed to reveal detectable IL-1 β expression (data not shown). Thus, the signaling cascades culminating in IL-1 β expression did not appear functional in the tumor cells. Overall, these data indicate that incorporating additional transcriptional factors, and additional signaling cascades into the model may improve the versatility and utility of the model.

4. Discussion

Previously we reported that varying the dose, length, or frequency of LPS treatment led to different TLR signaling responses in 4T1 and DC, and that this may have been related to differential expression of TLR4, CD14, MYD88 and TRAM [21]. We also found that, depending upon the conditions, TLR signaling could either enhance or suppress tumor growth [21]. Subsequently, we explored the effects of reducing TLR4 and MYD88 expression in mammary carcinoma and found that it led to slower tumor progression, and a decrease in CCL2 expression [22]. Because of the complexity of the TLR signaling cascade, and because this lack of

understanding can have serious implications if TLR signaling is modulated in a tumor setting where both types of cells are present, we set out to create a computational model of the TLR4 signaling cascade that could be used to gain a greater understanding of how this signaling cascade differs between tumor cells and normal white blood cells.

The term world in NetLogo was used to describe the modeled “cell” and its components. In the early stages we began with a base model made in a 2 dimensional (2D) world (the modeled cell). We then changed the model into 3D because the 2D world could not accommodate the amount of TLR4 on the cell surface, and the 3D system reflects a more accurate model of a cell where proteins are capable of moving along 3 dimensions. Protein motion was modeled as Brownian motion and was confirmed by tracking protein movement using “pen-down” to insure that movement was random and distributed throughout the cell. We also explored different sizes of the world and chose the dimensions that allowed distribution of proteins so that they did not overlap with one another. One goal for the model was versatility. For instance, the user could change the level of any signaling protein by changing the level in the NetLogo boxes or adjusting the sliders to regulate the amount of proteins recruited per signaling cascade. Thus, anyone could adjust the TLR signaling components to the level found in their particular cell line and then the model would show how much CCL2 would be produced upon exposure to a TLR agonist.

Once generated, the model was used to determine how much CCL2 DC and 4T1 would produce upon TLR signaling. In short, after adjusting the level of TAB3 we were able to generate data with the model that were similar to the experimental data. Incorporation of IRAKM as a negative

regulator of TLR signaling further improved the ability of the model to generate data that were more consistent with the experimental data. This negative feedback is particularly important for cells of the defense system such as DC since too much, or prolonged inflammation can be detrimental to the host [23,24]. The lack of IRAKM as a negative regulator for TLR signaling in 4T1 was also interesting because many tumors constitutively express pro-inflammatory proteins which contribute to the chronic inflammation associated with many cancers [25,26]. The lack of feedback inhibition in tumor cells may help explain these findings.

One aspect difficult to reconcile is that we used mRNA levels to predict protein levels. While we did not assess all of the proteins, we did directly compare mRNA and protein levels for NFκB and, with the exception of RELB, we found strong agreement between the numbers. The discrepancy with RELB may be due to the extremely low levels of this protein to begin with. Although more work is needed to determine how protein concentrations coincide with RNA levels for other proteins used in the model we believe qRT-PCR data is the most simple and automatic way to set the model parameters since it is reliable and widely available to biologists. While other methods (i.e. RNA Seq, western blot, generating cell lines with transcriptional reporter systems) can be used, these methods are slower, more costly, more variable between different labs, and not as widely available as qRT-PCR.

We identified several ways that the model may be further improved to provide more accurate predictions of CCL2 production. For instance, one way to improve the model would be to address where the proteins are located within the cell. For our model, we segregated proteins to the plasma membrane, cytoplasm, or nucleus allowing proteins to migrate

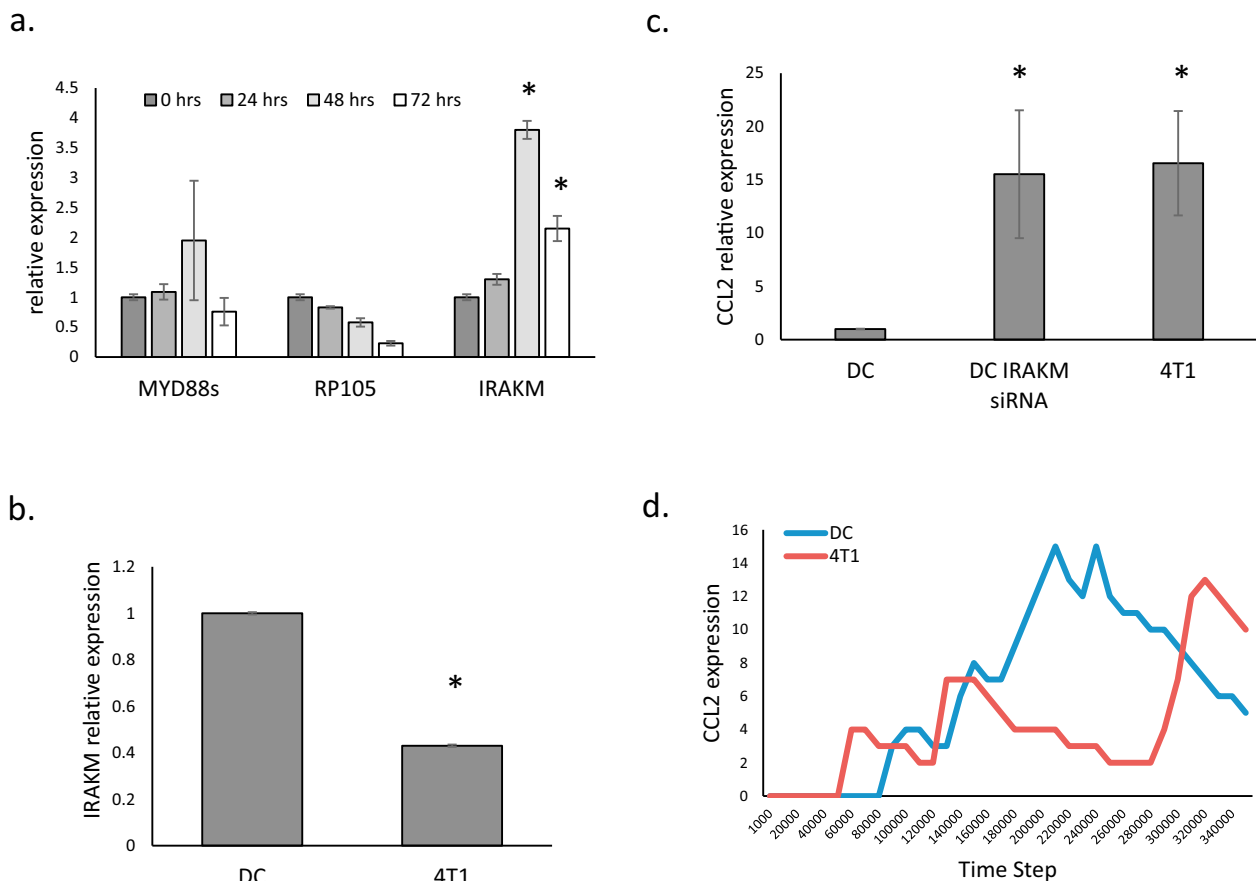


Fig. 6. Evaluating negative regulation of TLR signaling. (a) DC treated with LPS for 24–72 h were screened for expression of negative regulators of TLR signaling using qRT-PCR. (b) Expression of IRAKM was compared between 4T1 and DC after 72 h of LPS treatment. (c) After 72 h of LPS treatment CCL2 expression was quantified in DC, DC treated with siRNA specific for IRAKM, and 4T1. For all data *gapdh* was used as the reference gene, and untreated cells (a) or LPS treated DC (b, c) served as the control. The data represent the average and standard error of three separate experiments. Where indicated (*) $p < .05$ using Student's *t*-Test relative to control. (d) The model was run with IRAKM incorporated as a negative regulator of TLR signaling with the level of IRAKM in DC set to 600 and in 4T1 IRAKM was set to 60.

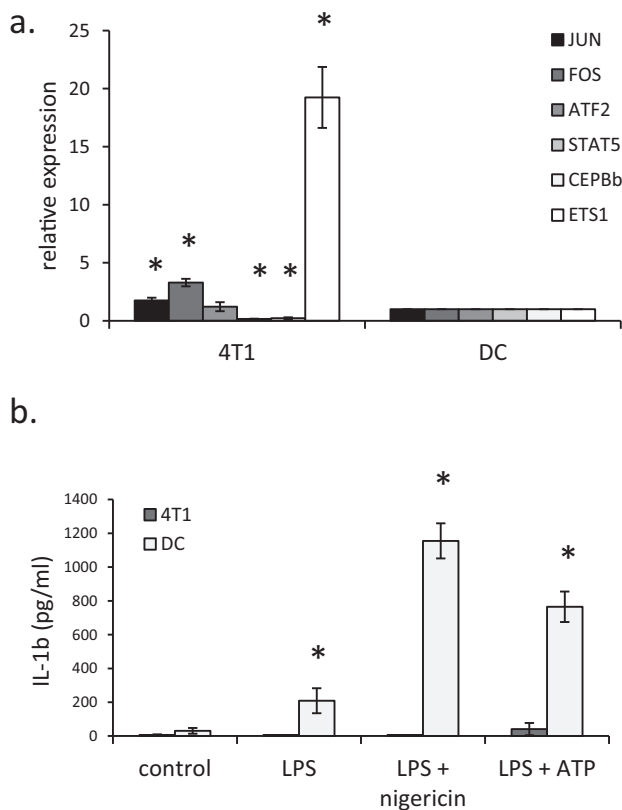


Fig. 7. Additional differences between 4T1 and DC that need to be incorporated into the model. (a) qRT-PCR was used to analyze expression of genes encoding additional CCL2 transcriptional factors with *gapdh* used as the reference gene and DC as the control. All data represent the average and standard error of at least three separate experiments. (b) In order to determine whether the findings were similar when cells were exposed to multiple signals 4T1 and DC were treated with LPS (10 ng/ml) for 72 h to prime the inflammasome and nigericin (20 μM) or ATP (5 mM) to activate the inflammasome, and then ELISA was used to quantitate the amount of IL-1β produced by the cells. Where indicated (*) $p < .05$ using Student's *t*-Test relative to DC (a) or control (b).

freely within these areas by Brownian movement. This approach is not optimal for all of the TLR signaling components which may be preferentially localized to particular areas of the cell. As a result, adding a cytoskeletal network and organelles would allow proteins to be localized to more confined regions of the cell and may also further improve the model. Perhaps the most critical and complex issue to address is the interactions between multiple signaling cascades. Our model did not take into account CCL2 transcriptional factors other than NFκB. JUN, FOS and ETS1 were expressed at significantly greater levels by the tumor cells than DC, while STAT5 and CEPBb were expressed at significantly lower levels. Determining the role of these transcriptional factors using gel shift assays and site directed mutagenesis would be crucial to determining the importance of these transcriptional factors for CCL2 production. Incorporation of such data may be used to generate an even more realistic model for TLR signaling. Yet, this would also require a much more sophisticated model which would allow multiple interconnected signaling cascades to interact. Indeed, our data, and the data of others, support the contention that signaling through two signaling cascades may result in a different response than a signal through one cascade. Since a cell would likely encounter multiple signals at any given time under normal conditions in vivo a computational modeling-based approach to evaluating how, and the extent to which multiple cascades interact may reveal a more complete understanding of cell signaling. We are currently working on a system that will allow this.

In summary, our model allows a user to change the level of any of the TLR signaling proteins and quickly learn how the altered protein levels

influence CCL2 expression. The data from the model was capable of recapitulating the data from the laboratory experiments. While developing the model we learned that NFκB, TAB3, and negative feedback were important for modeling CCL2 expression. The experimental data suggested that the tumor cells lacked negative regulation of TLR signaling. This is an area that requires further study because if similar results are found in additional tumor cell lines then these data may help explain why many tumors constitutively express pro-inflammatory cytokines and contribute to chronic inflammatory responses [25,26]. We are currently working on an experimental system that will allow us to stimulate and evaluate the outcome of multiple interconnected signaling cascades as well as a more versatile model that allows assessment of multiple interconnected signaling cascades. Overall, while we continue to improve the model, this study shows the practicality and utility of combining a modeling and experimental approach for unraveling signaling cascades.

Conflicts of interest

The authors report no conflicts of interest.

Disclosure

All authors contributed to the experiments and preparation of the article, and all authors have approved the final article.

Acknowledgements

This work was supported by a grant from the Howard Hughes Medical Institute to Lafayette College under the Precollege and Undergraduate Science Education Program, and by the Air Force Office of Scientific Research (grant FA9550-17-0293) to CWL. The Department of Biology and Lafayette College Excel Scholar program also supported this work.

Appendix A. Supplementary data

Supplementary data related to this article can be found at <https://doi.org/10.1016/j.combiomed.2017.12.013>.

References

- [1] B. Cheng, M. Lin, G. Huang, Y. Li, B. Ji, G.M. Genin, V.S. Deshpandes, T.J. Lu, F. Xu, Cellular mechanosensing of the biophysical microenvironment: a review of mathematical models of biophysical regulation of cell responses, *Phys. Life Rev.* (2017), <https://doi.org/10.1016/j.plrev.2017.06.016>.
- [2] W. Abou-Jaoude, P. Traynard, P.T. Monteiro, J. Saez-Rodriguez, T. Hellkar, D. Thieffry, C. Chauviya, Logical modeling and dynamical analysis of cellular networks, *Front Gen* (2016), <https://doi.org/10.3389/fgene.2016.00094>.
- [3] Z. Wang, J.D. Butner, R. Kerketta, V. Cristini, T.S. Diesboeck, Simulating cancer growth with multiscale agent-based modeling, *Semin. Canc. Biol.* (2015), <https://doi.org/10.1016/j.semcancer.2014.04.001>.
- [4] E. Klipp, W. Liebermeister, Mathematical modeling of intracellular signaling pathways, *BMC Neurosci.* 7 (Suppl 1) (2006).
- [5] D. Bray, R.B. Bourret, M.I. Simon, Computer simulation of the phosphorylation cascade controlling bacterial chemotaxis, *Mol. Biol. Cell* 4 (5) (1993) 469–482.
- [6] C.W. Liew, R. Kurt, A tool for developing agent based models of signaling cascades, in: *Proc 14th Eur Conf Artificial Life*, MIT Press, 2017. Sept:521–528.
- [7] C.L. Aslakson, F.R. Miller, Selective events in the metastatic process defined by analysis of the sequential dissemination of subpopulations of a mouse mammary tumor, *Canc. Res.* 52 (1992) 1399–1405.
- [8] H. Saji, M. Koike, T. Yamori, S. Saji, M. Seiki, K. Matsushima, M. Toi, Significant correlation of monocyte chemoattractant protein-1 expression with neovascularization and progression of breast carcinoma, *Cancer* 92 (2001) 1085–1091.
- [9] A. Lebrecht, C. Grimm, T. Lantzsche, E. Ludwig, L. Hefler, E. Ulbrich, H. Koelbl, Monocyte chemoattractant protein-1 serum levels in patients with breast cancer, *Tumor Biol.* 25 (2004) 14–17.
- [10] T. Ueno, M. Toi, H. Saji, M. Muta, H. Bando, K. Kuroi, M. Koike, H. Inadera, K. Matsushima, Significance of macrophage chemoattractant protein-1 in macrophage recruitment, angiogenesis, and survival in human breast cancer, *Clin. Canc. Res.* 6 (2000) 3282–3289.
- [11] G. Schreiber, J. Tel, K.H. Slieden, D. Benitez-Ribas, C.G. Figdor, G.J. Adema, I.J. de Vries, Toll-like receptor expression and function in human dendritic cell subsets:

- implications for dendritic cell-based and anti-cancer immunotherapy, *Canc. Immunol. Immunother.* 59 (2010) 1573–1582.
- [12] L. Hammerich, N. Bhardwaj, H.E. Kohrt, J.D. Brody, In situ vaccination for the treatment of cancer, *Immunotherapy* 8 (2016) 315–330.
- [13] E. Bonneau, Agent-based modeling: methods and techniques for simulating human systems, *Proc. Natl. Acad. Sci.* 99 (suppl 3) (2002) 7280–7287.
- [14] J. Yang, X. Meng, W.S. Hlavacek, Rule-based modeling and simulation of biochemical systems with molecular finite automata, *IET Syst. Biol.* 4 (6) (2010) 453–466.
- [15] M.A. Moreno Ayala, M.F. Gottardo, M.S. Gori, A.J. Nicola Candia, C. Carusco, A. De Laurentiis, M. Imsen, S. Klein, E. Bal de Kier Joffe, G. Salamone, M.G. Castro, A. Seilicovich, M. Candolfi, Dual activation of Toll-like receptors 7 and 9 impairs the efficacy of antitumor vaccines in murine models of metastatic breast cancer, *J. Canc. Res. Clin. Oncol.* (2017), <https://doi.org/10.1007/s00432-017-2421-7>.
- [16] S. Han, W. Xu, Z. Wang, X. Qi, Y. Wang, Y. Ni, H. Shen, Q. Hu, W. Han, Crosstalk between the HIF-1 and toll-like receptor/nuclear factor- κ B pathways in the oral squamous cell carcinoma microenvironment, *Oncotarget* 7 (2016) 37773–37789.
- [17] A. Del Prete, P. Allavena, G. Santoro, R. Fumarulo, M.M. Corsi, A. Mantovani, Molecular pathways in cancer-related inflammation, *Biochem. Med.* 21 (2011) 264–275.
- [18] N. Mukherjee, T.J. Houston, E. Cardenas, R. Ghosh, To be an ally or an adversary in bladder cancer: the NF- κ B story has not unfolded, *Carcinogenesis* 36 (2015) 299–306.
- [19] V. Ramesh, K. Selvarasu, J. Pandian, S. Myilsamy, C. Shanmugasundaram, K. Ganesan, NF κ B activation demarcates a subset of hepatocellular carcinoma patients for targeted therapy, *Cell. Oncol.* 39 (2016) 523–536.
- [20] X. Deng, M. Xu, C. Yuan, L. Yin, X. Chen, X. Zhou, G. Li, Y. Fu, C.A. Feghali-Bostwick, L. Pang, Transcriptional regulation of increased CCL2 expression in pulmonary fibrosis involves nuclear factor- κ B and activator protein-1, *Int. J. Biochem. Cell Biol.* 45 (2013) 1366–1376.
- [21] C. Palha De Sousa, C.M. Blum, E.P. Sgroie, A.M. Crespo, R.A. Kurt, Murine mammary carcinoma cells and CD11c+ dendritic cells elicit distinct responses to lipopolysaccharide and exhibit differential expression of genes required for TLR4 signaling, *Cell. Immunol.* 266 (2010) 67–75.
- [22] A.T. Egunsola, C.L. Zawislak, A.A. Akuffo, S.A. Chalmers, J.C. Ewer, C.M. Vail, J.C. Lombardo, D.N. Perez, R.A. Kurt, Growth, metastasis, and expression of CCL2 and CCL5 by murine mammary carcinomas are dependent upon Myd88, *Cell. Immunol.* 272 (2012) 220–229.
- [23] G.S. Schulert, A.A. Grom, Macrophage activation syndrome and cytokine-directed therapies, *Best Pract. Res. Clin. Rheumatol.* 28 (2014) 277–292.
- [24] R.V. D'Elia, K. Harrison, P.C. Oyston, R.A. Lukaszewski, G.C. Clark, Targeting the “cytokine storm” for therapeutic benefit, *Clin. Vaccine Immunol.* 20 (2013) 319–327.
- [25] M. Suarez-Carmona, J. Lesage, D. Cataldo, C. Gilles, EMT and inflammation: inseparable actors of cancer progression, *Mol. Online* 11 (2017) 805–823.
- [26] J. Li, F. Yang, F. Wei, X. Ren, The role of toll-like receptor 4 in tumor microenvironment, *Oncotarget* (2017) doi: 10.18632.